Available online at www.sciencedirect.com
SCIENCE DIRECT®
Carbohydrate Research 339 (2004) 569–578
Carbohydrate RESEARCH

Characterization of the crystalline structure of cellulose using static and dynamic FT-IR spectroscopy

Margaretha Åkerholm,[a] Barbara Hinterstoisser[b] and Lennart Salmén[a,*]

[a]*STFI, Swedish Pulp and Paper Research Institute, Box 5604, 114 86 Stockholm, Sweden*
[b]*BOKU—University of Natural Resources and Applied Life Sciences, Gregor Mendel Str. 33, A-1180 Vienna, Austria*

Received 23 June 2003; Received in revised form 18 September 2003; accepted 18 November 2003

Abstract—The cellulose structure is a factor of major importance for the strength properties of wood pulp fibers. The ability to characterize small differences in the crystalline structures of cellulose from fibers of different origins is thus highly important. In this work, dynamic FT-IR spectroscopy has been further explored as a method sensitive to cellulose structure variations. Using a model system of two different celluloses, the relation between spectral information and the relative cellulose I_α content was investigated. This relation was then used to determine the relative cellulose I_α content in different pulps. The estimated cellulose I allomorph compositions were found to be reasonable for both unbleached and bleached chemical pulps. In addition, it was found that the dynamic FT-IR spectroscopy technique had the potential to indicate possible correlation field splitting peaks of cellulose I_β.

Keywords: 2D FT-IR; Cellulose allomorphs; Crystallinity; Infrared spectroscopy; Chemical pulps

1. Introduction

The increased demand for an optimized fiber utilization in chemical pulping operations requires an in-depth understanding of the fiber material down to the ultrastructural level. The relationship between structural parameters such as cellulose crystallinity and the physical properties of pulp fibers is one aspect that has not been fully explored.[1] In order to better understand such relationships, methods for determining the cellulose crystal structure have to be further developed.

Crystalline native cellulose is composed of two different allomorphs, cellulose I_α and cellulose I_β,[2,3] where the monoclinic I_β allomorph is the most thermodynamically stable form. The allomorph composition has been found to be species specific. Due to the metastability of the triclinic I_α form, the allomorph composition may change during pulping.[4,5] The hydrogen-bonding pattern is different for the different cellulose allomorphs[6] and the mechanical properties ought therefore also to be different. A quantitative determination of the different allomorphs in various pulp fibers would therefore give information, which might explain differences in physical properties of these pulp fibers.

Characteristic IR absorption bands for the two allomorphs of native cellulose have earlier been identified both in the OH stretching region and in the 700–800 cm^{-1} region.[7] FT-IR spectroscopy has also been used to determine the allomorph compositions of cellulose I from different origins. Sassi et al.[8] used the deconvoluted bands of the OH stretching vibrations, whereas Imai and Sugiyama[9] determined the ratio of the absorption coefficients between 750 and 710 cm^{-1}. Yamamoto et al.[10] also used the 750 and 710 cm^{-1} peaks, but they carried out line-shape analyses of the spectra and then compared the ratios with the mass fractions determined by CP/MAS ^{13}C NMR. All these studies were made on highly ordered material such as *Cladophora*, *Valonia*, and bacterial celluloses, whose FT-IR spectra show more distinct bands than the spectra of wood celluloses.

* Corresponding author. Tel.: +46-8-6767-000; fax: +46-8-4115-518; e-mail: lennart.salmen@stfi.se

0008-6215/$ - see front matter © 2003 Elsevier Ltd. All rights reserved.
doi:10.1016/j.carres.2003.11.012

Dynamic FT-IR spectroscopy is known for its enhancement of spectral resolution due to an applied external mechanical perturbation of the system while recording the spectrum.[11] Since earlier studies had revealed differences in the dynamic FT-IR spectra of different pulps in the region of one characteristic cellulose I_β vibration,[12] it was judged to be of interest to investigate whether these differences could be quantitatively determined. The dynamic FT-IR technique has earlier also been shown to resolve the overlapping vibration bands of hydrogen bonds in spruce cellulose[13,14] and, since the main difference between the allomorphs of native cellulose is expected to be their hydrogen-bonding pattern, this technique was considered to be promising.

2. Materials and methods

2.1. Cellulose mixtures

In order to obtain a sample series with different proportions of cellulose I_α and cellulose I_β, two cellulose materials having different native compositions were mixed. Cotton linters was chosen as the I_β-rich cellulose and *Cladophora* sp. (algae) cellulose as the I_α-rich cellulose. The cotton linters was a commercially available grade (Crane AB, Sweden) and the *Cladophora* cellulose was prepared from naturally grown *Cladophora* sp.[15] Nine different samples with a cellulose I_α/I_β ratio ranging from 0.22 to 1.1 were prepared. CP/MAS ^{13}C NMR data was taken as the basis for the estimation of cellulose crystallinity in the mixtures as well as the cellulose I_α/I_β ratio.

Two samples were analyzed, pure cotton linters and a mixture of 45% *Cladophora* and 55% cotton linters. The pure cotton linters (A00) showed a cellulose crystallinity of 34% and a relative content of cellulose I_α in the crystalline part of 18%. Calculated from NMR data on the mixture (A45), the cellulose crystallinity of *Cladophora* was found to be 74% and the relative content of cellulose I_α in the crystalline part was 53% (Table 1).

Table 1. Cellulose samples used and their characteristics as determined by NMR

Cellulose sample	Composition (% *Cladophora*)	Crystallinity (calculated from NMR)	Cellulose I_α (% of crystalline part) (calculated from NMR)
A100	100	74	53
A50	50	54	42
A45	45	52	40
A40	40	50	39
A30	30	46	35
A20	20	42	30
A15	15	40	28
A10	10	38	25
A00	0	34	18

The shaded lines refer to samples for which the composition was determined by NMR measurements. The rest of the data are calculated from those values.

2.2. Pulps

Several available pulps with the chemical compositions shown in Table 2 were studied:

- An industrial spruce (*Picea abies*) *dissolving pulp* provided by Borregaard Chemcell, Norway.
- An industrially processed and *bleached* [OOQ(OP)Q (PO)] *softwood kraft pulp* with birch kraft pulp black liquor added to sorb xylan onto the fibers.
- An industrially pulped *kraft liner pulp*, mainly from pine (*Pinus sylvestris*), cooked to kappa no. 85. To remove most of the lignin, the pulp was treated with sodium chlorite in an acetate buffer at room temperature.
- An industrially batch-made unbleached *birch* (*Betula verrucosa*) *kraft pulp* with kappa no. 15.
- An unbleached, laboratory-made *acidic sulfite pulp* (pH 1.7) of Norway spruce (*P. abies*).

Table 2. Chemical composition of the investigated pulps

Pulp sample	Glucose (%)	Xylose (%)	Arabinose (%)	Mannose (%)	Galactose (%)	Klason lignin (%)	Pulp yield (%)
Dissolving pulp	98.1	1.0	<0.1	0.8	<0.1	0	
Bleached softwood kraft	84.4	10.3	0.4	4.8	0.1	0	
Kraft liner	77.8	10.8	1.7	8.8	0.9	3.0	
Birch kraft	68.5	30.7	0.2	0.5	0.1	0.4	
Acid sulfite	84.8	6.3	0.3	8.5	0.1	2.3	
Holocellulose	71.4	8.4	1.2	17.4	1.6	0.3	
FH kraft	92.7	4.4	<0.1	2.9	<0.1	0.5	42.9
RDH kraft	85.6	8.1	0.5	5.6	0.2	0.3	49.0
ITC kraft	84.8	8.1	0.5	6.4	0.2	0.3	50.4
PS kraft	82.0	7.3	0.5	9.9	0.4	0.2	53.5

- A *holocellulose* produced by chlorite delignification of chips of Norway spruce (*P. abies*) at 50 °C in an acetate buffer.

Four pulps that had been laboratory cooked using the same wood raw material [Norway spruce (*P. abies*)] but different modified kraft processes was also obtained. The intention had been to study possible differences in structure between fibers of the same origin processed in different ways. The following processes were used: FH (prehydrolyzed, heat treated in water before kraft cooking), RDH (rapid displacement heating technique), ITC (isothermal continuous cooking), and PS (polysulfide cooking). All four pulps were pulped to a target kappa number of 28 and the RDH, ITC, and PS pulps were then bleached in a D(E)D sequence to a target ISO brightness of 85%, while the FH pulp was chlorite delignified.

2.3. Sheets

Thin sheets (13–22 g/m^2) were made from the different cellulose mixtures and from the different pulps on a Formette Dynamique sheet former at 1400 rpm, giving sheets with the fibers oriented preferentially in the direction of rotation. Before sheet formation, the pulps were homogenized by pumping several times through a slit in a laboratory homogenizer (Gaulin Corp., Everett, MA, USA).

2.4. Static FT-IR measurements

All spectra were recorded using a FTS 6000 FT-IR spectrometer (Digilab, Randolph, MA, USA). The static IR spectra (4000–400 cm^{-1}) used for crystallinity determinations were recorded using a deuterated tri-glycerine sulfate (DTGS) detector. Thirty two scans with a resolution of 8 cm^{-1} were co-added. These spectra were normalized at 2900 cm^{-1} (C–H stretching vibration). The IR crystallinity ratios plotted in Figure 1 were calculated from two such measurements for each sample and a mean ratio was thereafter calculated. Since the location of the characteristic peak maximum varied somewhat between the samples, the height was determined at slightly different wave numbers. For H_{1429} the maximum varied between 1423 and 1429 cm^{-1}, for H_{1372} it varied between 1354 and 1370 cm^{-1}, and for H_{2900} it varied between 2897 and 2900 cm^{-1}.

2.5. Dynamic FT-IR measurements

For the dynamic FT-IR measurements, samples 25 × 30 mm in size were cut from the oriented fiber sheets (30 mm in the fiber direction) and mounted in a polymer modulator (Manning Applied Technologies Inc., Troy, ID, USA). Samples were mounted with the fibers oriented parallel to the stretching direction. Before the start of each measurement, the samples were prestretched and dried inside the purged sample compartment until dry conditions (0% relative humidity) were reached. A small sinusoidal strain (<0.3%) with a frequency of 16 Hz was then applied to the sample and the transition dipole responses were monitored as a phase lag with respect to the external perturbation. With the aid of a KRS5 wire grid polarizer, the incident IR radiation was polarized 0° (parallel) to the stretching direction (an example of a 90° polarized measurement is also shown in Figure 12). The interferometer was run in a step-scan mode with a scanning speed of 0.5 Hz and a phase modulation of 400 Hz using a liquid-nitrogen-cooled MCT (mercury cadmium telluride) detector. An undersampling ratio of 4 was used together with an optical long-pass filter to reduce the spectral range to 3950–700 cm^{-1}. Four scans with a resolution of 8 cm^{-1} were co-added in each measurement and the required measurement time was about 2.5 h (the pure *Cladophora* sample was also

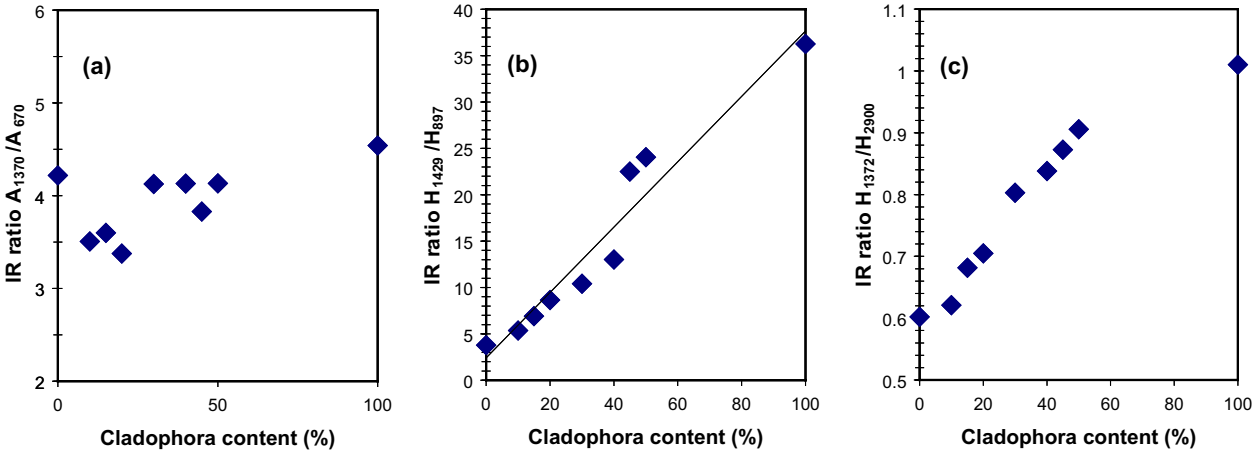

Figure 1. Three different IR ratios plotted against the composition of the mixed cellulose samples: (a) A_{1370}/A_{670}, (b) H_{1429}/H_{897}, (c) H_{1372}/H_{2900}.

measured with a resolution of 2 cm^{-1}). Since the phase of the external perturbation in relation to the interferometer steps was known, it was possible to use digital signal processing to extract the dynamic changes in the IR transmission spectrum of the sample from the detector signal. The interferograms obtained were Fourier transformed and a triangular apodization function[16] was applied. The resulting in-phase and out-of-phase spectra were divided by the static spectrum and thereafter baseline corrected.

The dynamic spectra shown in Figures 2, 5, and 9 are mean spectra of three measurements and the spectra in Figure 10 are mean spectra of five measurements. Before averaging, the dynamic spectra were normalized as follows. The spectral result from each measurement was divided into one phase spectrum (phase delay of each absorption band) and one magnitude spectrum (the amount of induced absorption change for each absorption band). All magnitude spectra were then normalized to 1.0 at 1435 cm^{-1}, a HOC bending, which has the same relative strain response as the C–O–C asymmetric bridge stretching (1169 cm^{-1}),[17] and new in-phase and out-of-phase spectra were calculated from these. The reason for not normalizing at 1169 cm^{-1} was that some of the samples showed too high an absorption in this area. The normalized in-phase spectra were then used for the peak height calculations, which were required for the cellulose I_α estimation. The estimates in Table 3 are means of 3–5 measurements. The mean dynamic spectra were used only for the illustrations in Figures 2, 5, 9, and 10.

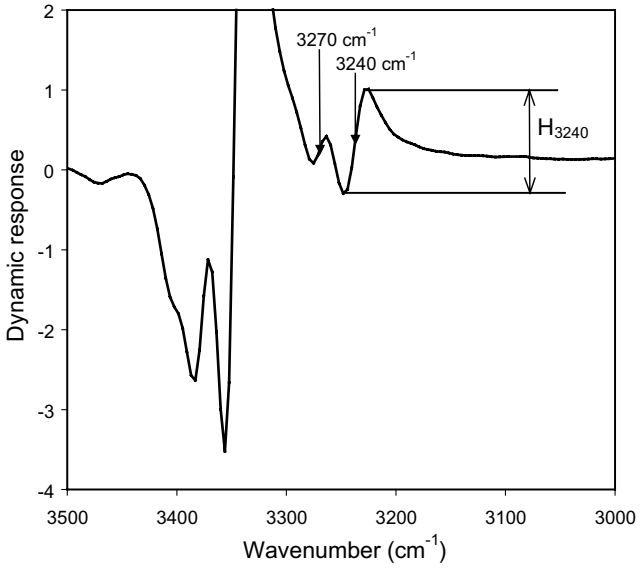

Figure 2. Dynamic in-phase mean spectrum of one cellulose mixture in the region from 3000 to 3500 cm^{-1}.

3. Results

3.1. Crystallinity

As a calibration of the allomorph quantification, a series with mixtures of celluloses having known allomorph compositions was used in this study. For this series, the cellulose crystallinity was investigated using different IR crystallinity ratios reported in the literature.[18–20] Three different IR ratios are plotted for the series of mixed cellulose samples in Figure 1. These different peak height and peak area ratios were measured in the static absorbance spectra of the cellulose mixtures.

The IR ratio A_{1370}/A_{670} was used by Richter et al.[18] to study the conversion of cellulose I into cellulose II during alkaline treatment. This is the ratio of the area of the IR peaks between 1300 and 1400 cm^{-1} to the area of the IR peak at 670 cm^{-1}. The rather constant value of this IR ratio found through the series of mixed native celluloses (Fig. 1a) indicates that this ratio does not measure the

Table 3. Cellulose IR crystallinity ratios and estimations of relative content of cellulose I_α in pulps (numbers in parentheses are the standard deviations)

Pulp sample	IR crystallinity ratio[a]			Estimated relative content of cellulose I_α (%)
	A_{1370}/A_{670}	H_{1429}/H_{897}	H_{1372}/H_{2900}	
Dissolving pulp	4.7 (0.1)	3.4 (0.1)	0.92 (0.06)	21 (2.0)[b]
Bleached softwood kraft	6.1 (0.3)	2.4 (0.03)	0.78 (0.02)	51 (2.8)[b]
Kraft liner	6.4 (0.04)	2.4 (0.05)	0.75 (0.04)	50 (5.7)[b]
Birch kraft	7.7 (0.1)	1.5 (0.03)	0.77 (0.01)	46 (0.9)[b]
Acid sulfite	7.2 (0.1)	2.8 (0.1)	0.84 (0.02)	59 (0.9)[b]
Holocellulose	6.9 (0.3)	2.7 (0.1)	0.86 (0.02)	57 (0.4)[b]
FH kraft	4.1 (0.3)	3.5 (0.3)	0.79 (0.02)	40 (6.2)[c]
RDH kraft	5.1 (0.1)	3.0 (0.1)	0.77 (0.01)	46 (3.4)[c]
ITC kraft	4.9 (0.5)	3.1 (0.3)	0.78 (0.01)	47 (9.8)[c]
PS kraft	5.4 (0.3)	3.1 (0.3)	0.76 (0.02)	46 (2.8)[c]

[a]The crystallinity ratios are mean values of two measurements.
[b]Estimates based on three measurements.
[c]Estimates based on five measurements.

cellulose crystallinity but rather the cellulose I/cellulose II ratio. The IR ratios H_{1429}/H_{897} and H_{1372}/H_{2900} are ratios between different peak heights, 1429–897[19] and 1372–2900 cm^{-1},[21] respectively. The IR ratio H_{1429}/H_{897} was linearly related to the amount of *Cladophora* cellulose in the mixtures (Fig. 1b) and this can be taken as an indication that the sample preparation of the native cellulose mixtures was successful. The H_{1429}/H_{897} ratio for these pure cellulose mixtures ranged from 3.7 to 39, whereas the same IR ratio for the pulps studied varied only from 1.5 to 5.0 (Table 3). The IR ratio H_{1372}/H_{2900} gave a linear relation (0.6–0.9) for the mixtures containing up to 50% *Cladophora* cellulose. Thereafter a leveling out toward the value for the pure *Cladophora* cellulose seemed to occur (Fig. 1c). Values greater than 1 for the IR ratio H_{1372}/H_{2900} of cellulose samples have not been found in the literature. For the pulps, this IR ratio varied between 0.68 and 0.92 (Table 3).

3.2. Cellulose I_α and I_β allomorphs

The allomorph composition of cellulose I was investigated using dynamic FT-IR spectroscopy. Dynamic FT-IR spectra display the changes occurring at each wave number in the static spectra while the sample is subjected to dynamic strain.[11] This means that dynamic peaks appear when the intensity of a peak increases or decreases as a result of the applied perturbation. So-called split dynamic peaks appear when the energy of the vibration is changed when the polymer is strained.[22] The dynamic spectral results are also two dimensional (2D FT-IR) in that they have one elastic and one viscous component. Under the dry conditions prevailing in the present measurements, the cellulose is in its glassy state and therefore elastic in nature. The viscous component (out-of-phase spectrum) of the dynamic FT-IR spectrum is thus almost zero in such measurements. Only the in-phase spectra, representing the elastic part of the dynamic spectra, are therefore shown in this paper. The possibility of resolving the OH stretching region of spruce cellulose by using dynamic FT-IR spectroscopy was demonstrated earlier.[13,14] A corresponding spectrum of one of the pure cellulose mixtures is plotted in Figure 2. The bands characteristic of cellulose I_α and cellulose I_β in the OH region are reported to be found at 3240 and 3270 cm^{-1},[7] respectively. These two wave numbers are marked in Figure 2, where it can be seen that in each case there is one positive peak to the right and one negative peak to the left. These are examples of the split dynamic peaks mentioned above. A correlation was found between the peak-to-valley intensity of the I_α characteristic peak at 3240 cm^{-1} and the cellulose I_α allomorph content (Fig. 3). This correlation was only linear for the mixed samples, not for the samples of pure cotton linters or for pure *Cladophora*. When dynamic FT-IR spectra of chemical pulps were investigated, the resolution was found to be much lower in this region than for the pure celluloses, and it was not possible to achieve any quantitative evaluation of the pulps.

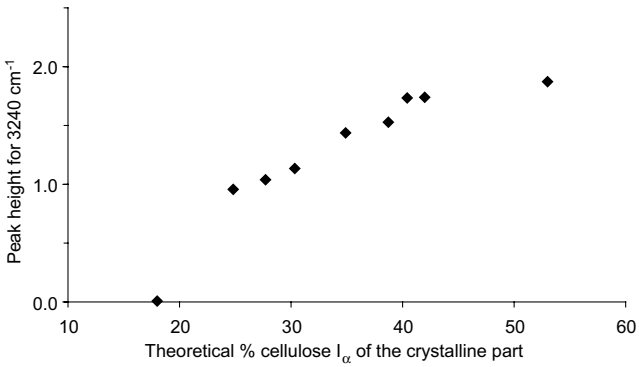

Figure 3. The peak intensity of the 3240 cm^{-1} peaks plotted against the calculated (from NMR) I_α fraction of the crystalline cellulose for the cellulose mixtures.

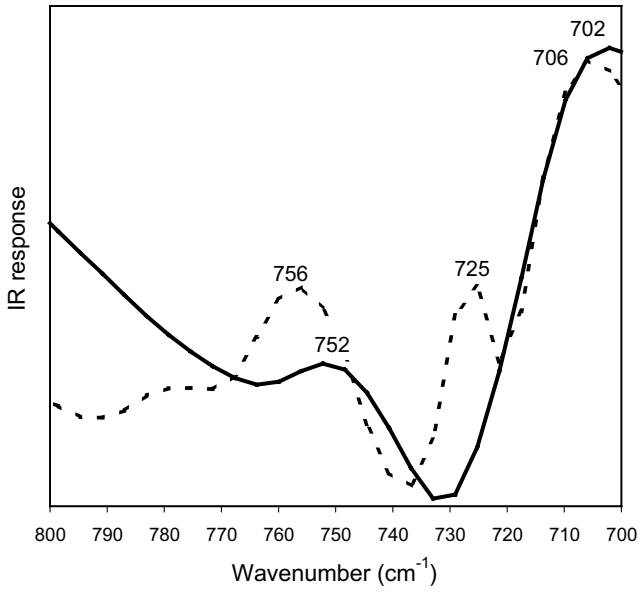

Figure 4. Comparison of static and dynamic in-phase FT-IR spectra of one cellulose mixture from 700 to 800 cm^{-1}. Solid line = static spectrum and broken line = dynamic in-phase spectrum. Cellulose I_α is characterized by the absorption peak at 750 cm^{-1}, while cellulose I_β has its characteristic peak at 710 cm^{-1}.

Figure 4 shows the static and dynamic in-phase spectra of the same cellulose mixture in the low-wave number region where characteristic peaks for cellulose I_α and cellulose I_β are to be found.[7] The weak static peak at 750 cm^{-1}, characteristic for cellulose I_α, was better resolved in the dynamic spectrum and the maximum was shifted to a slightly higher wave number. The static peak characteristic of cellulose I_β at 710 cm^{-1} was also present in the dynamic spectrum and the dynamic spectrum also contained a third peak at 725 cm^{-1}.

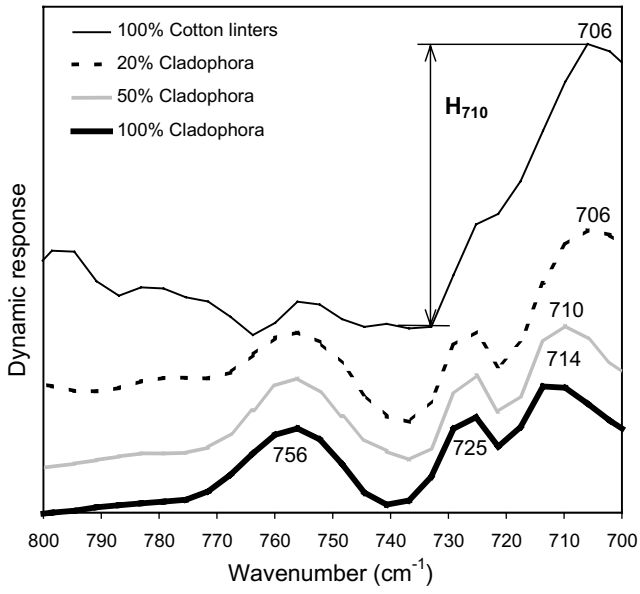

Figure 5. Dynamic in-phase mean spectra of different cellulose mixtures from 700 to 800 cm^{-1}. The spectra are plotted with different offsets.

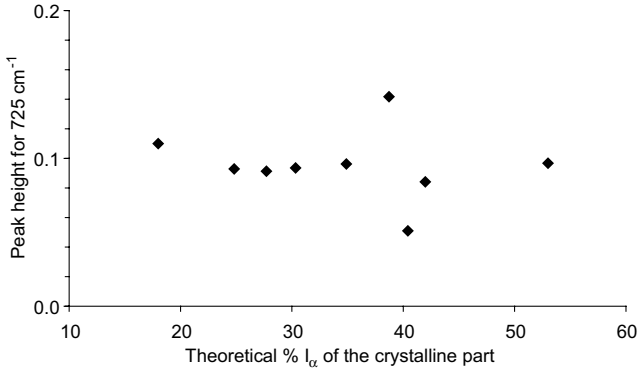

Figure 6. The peak intensity of the 725 cm^{-1} peaks plotted against the calculated (from NMR) I_α fraction of the crystalline cellulose for the cellulose mixtures.

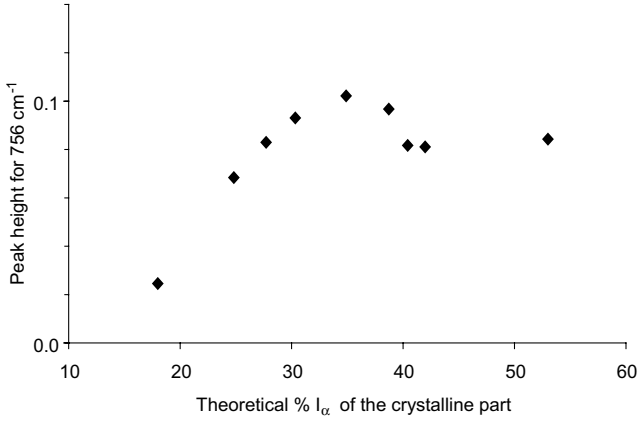

Figure 7. The peak intensity of the 756 cm^{-1} peaks plotted against the calculated (from NMR) I_α fraction of the crystalline cellulose for the cellulose mixtures.

Dynamic spectra of four cellulose mixtures are compared in Figure 5. It can be seen that all these spectra contained the three peaks mentioned in this wave number region. The peaks at 725 and 756 cm^{-1} both remained at constant wave number and their intensity change through the series of cellulose mixtures is shown in Figures 6 and 7. It is evident in Figure 6 that the intensity of the 725 cm^{-1} peak was fairly constant through the series, revealing no dependence on the allomorph composition of the material. The intensity of the 756 cm^{-1} peak (Fig. 7) showed a linear correlation to the allomorph composition for the cotton-linters-rich samples but the intensity was constant from 35% to 100% *Cladophora* in the sample. In contrast, the peak maximum at about 710 cm^{-1} changed rather linearly in both intensity and wave number position (Fig. 5) with the proportion of *Cladophora* cellulose in the mixture. Sugiyama et al. also found different IR peak maxima for this peak depending on species.[7] In Figure 8, the peak intensity of the 710 cm^{-1} peaks is plotted against the I_α portion of the crystalline cellulose. The peak intensity was calculated as the maximum intensity between 702 and 714 cm^{-1} minus the minimum intensity between 735 and 745 cm^{-1}, illustrated in Figure 5. The relationship in Figure 8 was fitted with a coefficient of determination ($R^2 = 0.89$) to

$$\%I_\alpha = (H_{710} - 0.3655)/(-0.004783) \qquad (1)$$

where H_{710} is the peak height of the 710 cm^{-1} peak in the dynamic in-phase spectrum from a magnitude spectrum normalized to 1.0 at 1435 cm^{-1}. As expected, a negative correlation was found since the 710 cm^{-1} peak is a characteristic of cellulose I_β.

Figure 9 shows the dynamic in-phase spectra of the same wave number region for several wood fiber pulps, ranging from a dissolving pulp to a holocellulose. These spectra are rather different from the spectra of the pure cellulose mixtures. Instead of being dominated by the peak at about 710 cm^{-1}, these spectra are dominated by

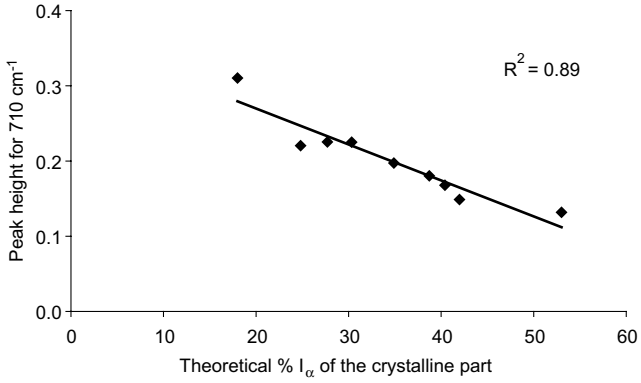

Figure 8. The peak intensity of the 710 cm^{-1} peaks plotted against the calculated (from NMR) I_α fraction of the crystalline cellulose for the cellulose mixtures.

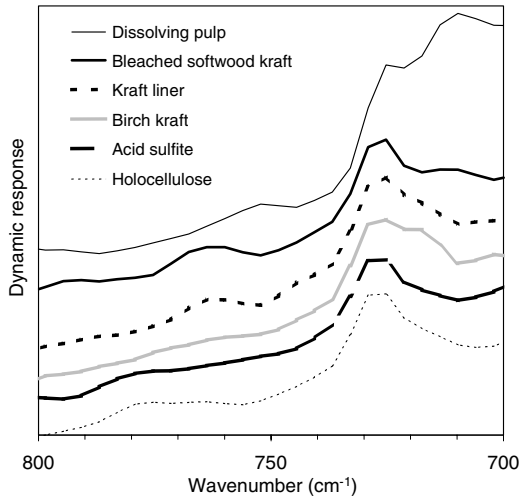

Figure 9. Dynamic in-phase mean spectra of different pulps from 700 to 800 cm^{-1}. The spectra are plotted with different offsets.

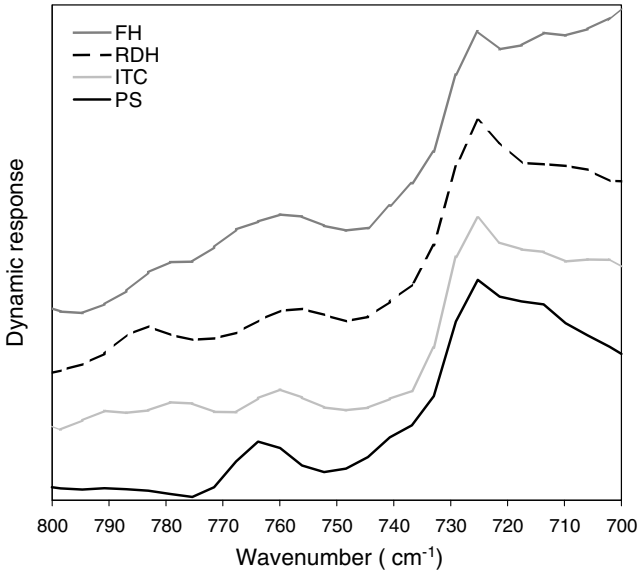

Figure 10. Dynamic in-phase mean spectra of four different bleached laboratory cooked kraft pulps from 700 to 800 cm^{-1}. The spectra are plotted with different offsets.

the 725 cm^{-1} peak, except for the dissolving pulp. The spectrum of the dissolving pulp resembles the spectrum of cotton linters, indicating a high content of cellulose I_β in this pulp. The 710 cm^{-1} peak was not so well resolved in the other pulp spectra and the maximum varied from 706 to 718 cm^{-1}. In the birch kraft pulp, two maxima could be seen in this region. The well-resolved cellulose I_α peak at 756 cm^{-1} in the pure cellulose mixtures was not seen in the pulps. The two softwood kraft pulps had instead a peak at 764 cm^{-1}, and the holocellulose and acid sulfite pulp had a weak peak at 779 cm^{-1}. In general, it can be seen that the spectrum of the acid sulfite pulp resembled the spectrum of the holocellulose more than the spectrum of the kraft pulps. The birch kraft pulp differed from the softwood kraft pulps by a more resolved cellulose I_β peak at 718 cm^{-1} and no peak at 764 cm^{-1}. This was probably due to the fact that birch wood is more enriched in the cellulose I_β allomorph while softwoods are more enriched in the cellulose I_α allomorph.[23]

From the spectra in Figure 9, the relative proportion of cellulose I_α in the pulps was estimated by inserting the calculated peak height for 710 cm^{-1} as defined earlier (H_{710}) for each pulp into Eq. 1. The values listed in Table 3 are the mean values of three measurements with the standard deviation in parentheses. The holocellulose and the acid sulfite pulp were found to have the highest proportion of cellulose I_α, whereas the dissolving pulp had the lowest proportion (rich in cellulose I_β). The birch kraft pulp had less cellulose I_α than the softwood kraft pulps.

The dynamic in-phase spectra of the four differently cooked laboratory kraft pulps over the 700–800 cm^{-1} region are compared in Figure 10. The estimation of the relative cellulose I_α content (Table 3) gave a lower value for the FH pulp than for the other three pulps. All these pulps have a lower estimated proportion of cellulose I_α than the industrially cooked softwood kraft pulps. The four spectra of Figure 10 differ in both the cellulose I_β and cellulose I_α regions of the IR spectrum. The PS pulp with the highest content of glucomannan had a well-resolved peak at 764 cm^{-1}, while the other pulps had additionally peaks at about 780 cm^{-1}. In the cellulose I_β region, the RDH pulp had its peak maximum at 710 cm^{-1}, while the other three pulps had the maximum at 714 cm^{-1}. Common for all pulps (Figs. 9 and 10) was the dominance of the 725 cm^{-1} peak as well as the appearance of a peak at about 760 cm^{-1} for all the softwood kraft pulps.

4. Discussion

The different IR ratios for estimating cellulose crystallinity used in this study[18–21] were all empirically developed by studying changes in IR spectra in relation to changes in crystallinity measured by different methods such as X-ray. Such correlations should always be treated with caution when the reason for the correlation is not understood. In vibrational spectra, three types of so-called regularity peaks exists.[24] One type characterizes conformational regularity such as *trans*/*gauche* isomerism, the second type is associated with long stereoregular chain segments such as helical structures and the last type consists of true crystallinity peaks. True crystallinity peaks are a consequence of inter-chain interactions characteristic for three-dimensional order in the crystal and are absent in the amorphous phase of the polymer. If the second type of peak is used for

crystallinity determinations, only the order along the chain direction will be measured. An additional problem when trying to measure polymer crystallinity is the existence of states of order intermediate between the truly crystalline state and the truly amorphous phase, which is indeed true of native cellulose.[15] The very different correlations found between the investigated IR ratios and the *Cladophora* content of the mixtures (Fig. 1) reveal that the selected IR bands originate from different types of regularity peaks. In addition, the values for the pulps varied greatly between the different ratios and also within different intervals than for the cellulose mixtures. It has been deduced that the ratio H_{1429}/H_{897} describes the lateral order,[25] that is, crystalline packing of the chains, and the small variation in this ratio found for the pulps compared with the cellulose mixtures could possibly be explained by the much larger fibrils in the *Cladophora* cellulose than in wood cellulose.[15]

The interpretation of the dynamic FT-IR spectrum of cellulose in the area 700–800 cm^{-1} is not straightforward since some peaks are present, which are not assigned in the static FT-IR spectrum. There are also different assignments in the literature of the two allomorph-characteristic peaks at 710 and 750 cm^{-1}. These vibrations were referred to by Atalla as O–H out-of-plane bending,[26] whereas Blackwell et al.[27] proposed that the band at 750 cm^{-1} is a CH_2 rocking vibration, while Sugiyama et al.[7] left the assignments open. For polymers in general, CH_2 rocking vibrations are reported in this region with the most intense in-phase band at 724 ± 4 cm^{-1},[28,29] interestingly at the same position as the 'extra' peak in the parallel polarized dynamic FT-IR spectrum (Fig. 4). However, the O–H out-of-plane vibrations are sensitive to changes in hydrogen bonding[29] and they may therefore be characteristic of the two allomorphs of cellulose I. The different relations between the intensities of the peaks at 710 and 756 cm^{-1} and the cellulose I allomorph composition (Figs. 7 and 8) point to different assignments of the two peaks. Very different IR absorption coefficients have also been reported for these peaks.[9] For crystalline polymers with more than one molecule per unit cell, a splitting (crystal splitting or correlation field splitting) of key vibrational modes may appear.[24,28,29] Atalla drew the conclusion that there is only one molecule per unit cell in both cellulose I_α and cellulose I_β due to the absence of such a splitting in the Raman spectrum of *Halocynthia*.[26] This crystal splitting effect is not always noticed because of weak inter-chain interactions in the crystal, and the broadness of the bands can obstruct the resolution of such a splitting. The size of the splitting is larger for vibrations directed perpendicular to the backbone of the polymer than for vibrations directed along the backbone. One method for observing crystal splitting is to cool the sample.[24] It is possible that, during the straining of the polymers in a dynamic FT-IR measurement, the chains come closer to each other and that this can result in stronger inter-chain interactions that cause crystal splitting. A high-resolution (2 cm^{-1}) dynamic in-phase spectrum of *Cladophora* is shown in Figure 11 for the CH bending region. In this spectrum, four resolved peaks can be seen at 1379, 1374, 1363, and 1358 cm^{-1}, whereas neither deconvoluted[30] nor second derivative[31] FT-IR spectra of native celluloses have shown more than two peaks in the area. This shows that it is possible to observe crystal splitting in the dynamic FT-IR spectra of highly crystalline samples. This may be the phenomenon responsible for the two peaks observed at 710 and 725 cm^{-1}, due to the unit cell of cellulose I_β, which is made up of two molecules. The distance between the two bands (15 cm^{-1}) is also consistent with the splitting of bands in crystalline polyethylene with two molecules per unit cell.[24] In contrast, there is only one peak at 756 cm^{-1} corresponding to the unit cell of cellulose I_α, which is made up of one molecule. There is however still a question as to why the 725 cm^{-1} peak does not change linearly in intensity with the allomorph composition like the 710 cm^{-1} peak does. The shape of the dynamic spectra of the pulps (Figs. 9 and 10) indicates that there may be more peaks, which are unresolved between 700 and 720 cm^{-1}. The polarization of the 710 and 750 cm^{-1} bands has also been questioned[7] and found to change upon annealing. Figure 12 shows that this crystal splitting of the dynamic spectrum occurs only in the 0° and not in the 90° polarization spectrum.

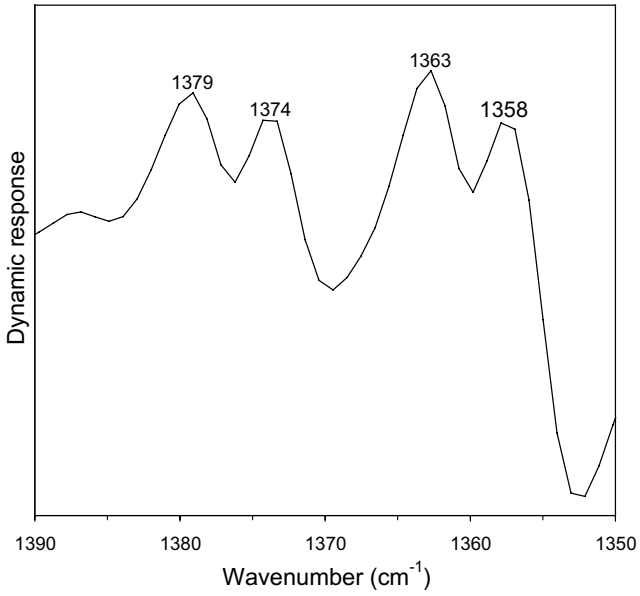

Figure 11. Dynamic in-phase spectra of *Cladophora* cellulose recorded with a resolution of 2 cm^{-1} in the region from 1350 to 1390 cm^{-1}.

In the IR spectrum of *n*-nonadecane, split crystallinity bands appear between 740 and 780 cm^{-1} in the orthorhombic phase. These change to single bands in the α phase and disappear in the melted state.[28] The differences in the dynamic spectra of the pulps in the

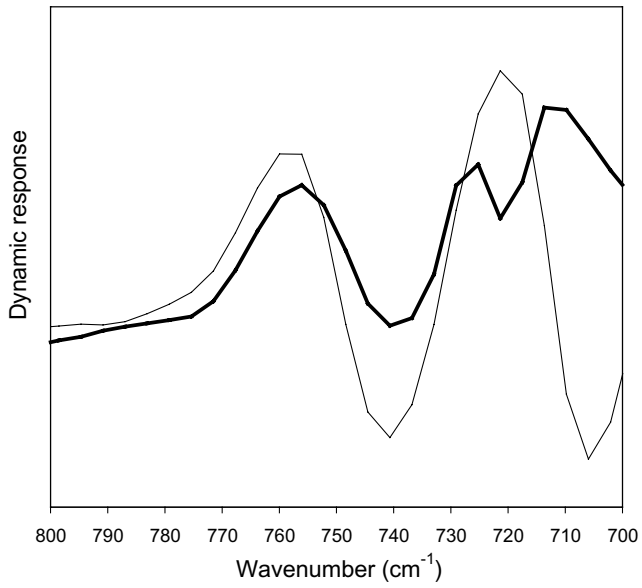

Figure 12. Dynamic in-phase spectra at 0° polarization (thick line) and at 90° polarization (thin line) of *Cladophora* cellulose in the region from 700 to 800 cm^{-1}.

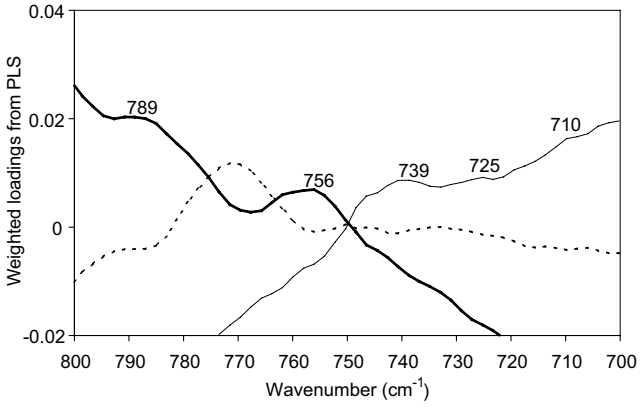

Figure 13. Weighted loadings from a PLS analyses of alkali-extracted holocelluloses. The thin solid line represents cellulose, the thick solid line represents glucomannan, and the broken line represents xylan. The values of loadings show the contribution from each polymer to the IR absorption in the area.

same region (Figs. 9 and 10) might also be a consequence of different inter-chain interactions between the fibrils in the different pulps. The different aggregations of fibrils during pulping[32–34] could give these different interactions. A PLS analysis of a series of extracted holocelluloses[35] has shown that the hemicelluloses contribute less to the spectra between 700 and 750 cm^{-1} than between 750 and 800 cm^{-1}, see Figure 13. The differences between 750 and 800 cm^{-1} in Figures 9 and 10 might thus also be attributed to differences in the molecular order of the hemicelluloses or differences in the interactions between the polysaccharides. Larsson and co-workers[4,34,36] have shown that the hemicelluloses contribute to the C-4 signal of the CP/MAS ^{13}C NMR spectrum of different pulps but not in the spectrum of holocellulose because of differences in the interactions between the polysaccharides. There was one hemicellulose signal from the birch kraft pulps, two signals from spruce kraft pulps, and no discernible hemicellulose signals maxima from the spruce sulfite pulps in the NMR spectra.

Since the estimates of the cellulose I allomorph composition reported in this paper are based on CP/MAS ^{13}C NMR data of *Cladophora* and cotton cellulose, the absolute values may differ if other methods such as X-ray are used or if other forms for comparison, such as direct NMR measurements on the pulps, are adopted. With the dynamic FT-IR method, clear differences were detected between differently processed fibers such as acid sulfite and kraft pulps. The decrease in the relative amount of cellulose I_α after kraft pulping was in agreement with the results of earlier NMR studies.[5,37] The reason for the change in the proportion of cellulose I_α is that the cellulose I_β form is more thermodynamically stable and that a conversion from cellulose I_α to cellulose I_β thus occurs at the high temperature and high alkalinity prevailing during the kraft process. The acid sulfite pulping process does not seem to affect the allomorph conversion in the same way, as has earlier been revealed by NMR.[4] The reason could be that this transformation is affected both by the temperature and by the medium, where an alkaline medium is more favorable for the transformation.[38]

5. Conclusions

A new method based on dynamic FT-IR spectroscopy for the estimation of the cellulose I allomorph composition in pulp samples is presented. The higher resolution in the spectra as a consequence of the sensitivity of dynamic FT-IR spectroscopy to structural differences in polymers makes this analysis possible. There are nevertheless still spectral features in the vibrational spectrum of cellulose, which remain to be explained.

Acknowledgements

The authors thank adj. Prof. T. Iversen and Dr. T. Larsson for performing the NMR measurements and for supplying the *Cladophora* and cotton celluloses. WURC (Wood Ultrastructure Research Center, SLU, Uppsala) is acknowledged for the use of the differently processed kraft samples. Part of this work (M. Åkerholm) was carried out within the framework of wood and wood fiber, a post-graduate school sponsored by the Swedish Council for Forestry and Agricultural Research and the Swedish University of Agricultural Sciences. Anthony Bristow is acknowledged for the linguistic revision.

References

1. Horii, F. Structure of Cellulose: Recent Developments in its Characterization. In *Wood and Cellulosic Chemistry*; Hon, D. N.-S., Shiraishi, N., Eds.; 2nd ed.; Marcel Dekker: New York, 2001; pp 83–107.
2. VanderHart, D. L.; Atalla, R. H. *Macromolecules* **1984**, *17*, 1465–1472.
3. Atalla, R. H.; VanderHart, D. L. *Science* **1984**, *223*, 283–285.
4. Hult, E.-L.; Larsson, P. T.; Iversen, T. *Holzforschung* **2002**, *56*, 179–184.
5. Maunu, S.; Liitiä, T.; Kauliomäki, S.; Hortling, B.; Sundquist, J. *Cellulose* **2000**, *7*, 147–159.
6. Sugiyama, J.; Yuong, R.; Chanzy, H. *Macromolecules* **1991**, *24*, 4168–4175.
7. Sugiyama, J.; Persson, J.; Chanzy, H. *Macromolecules* **1991**, *24*, 2461–2466.
8. Sassi, J.-F.; Tekely, P.; Chanzy, H. *Cellulose* **2000**, *7*, 119–132.
9. Imai, T.; Sugiyama, J. *Macromolecules* **1998**, *31*, 6275–6279.
10. Yamamoto, H.; Horii, F.; Hirai, A. *Cellulose* **1996**, *3*, 229–242.
11. Noda, I.; Dowrey, A. E.; Marcott, C. Two-Dimensional Infrared (2D IR) Spectroscopy. In *Modern Polymer Spectroscopy*; Zerbi, G., Ed.; Wiley-VCH: Weinheim, 1999; pp 1–32.
12. Åkerholm, M.; Salmén, L. *J. Pulp Pap. Sci.* **2002**, *28*, 245–249.
13. Hinterstoisser, B.; Salmén, L. *Vib. Spectrosc.* **2000**, *22*, 111–118.
14. Hinterstoisser, B.; Salmén, L. *Cellulose* **1999**, *6*, 251–263.
15. Wickholm, K.; Larsson, P. T.; Iversen, T. *Carbohydr. Res.* **1998**, *312*, 123–129.
16. Griffiths, P. R.; Haseth, J. A. d. *Fourier Transform Infrared Spectroscopy*; Wiley-Interscience: New York, 1986.
17. Hinterstoisser, B.; Åkerholm, M.; Salmén, L. *Carbohydr. Res.* **2001**, *334*, 27–37.
18. Richter, U.; Krause, T.; Schempp, W. *Angew. Makrolmol. Chem.* **1991**, *185/186*, 155–167.
19. O'Connor, R. T.; DuPeé, E. F.; Mitchum, D. *Textile Res. J.* **1958**, *28*, 382–392.
20. Nelson, M. L.; O'Connor, R. T. *J. Appl. Polym. Sci.* **1964**, *8*, 1311–1324.
21. Nelson, M. L.; O'Connor, R. T. *J. Appl. Polym. Sci.* **1964**, *8*, 1325–1341.
22. Bretzlaff, R. S.; Wool, R. P. *Macromolecules* **1983**, *16*, 1907–1917.
23. Newman, R. H. *J. Wood Chem. Technol.* **1994**, *14*, 451–466.
24. Bower, D. I.; Maddams, W. F. *The Vibrational Spectroscopy of Polymers*; Cambridge University Press: Cambridge, 1989.
25. Hurtubise, F. G.; Krässig, H. *Anal. Chem.* **1960**, *32*, 177–181.
26. Atalla, R. H. Celluloses. In *Comprehensive Natural Products Chemistry*; Barton, D., Nakanishi, K., Meth-Cohn, O., Eds.; 1st ed.; Elsevier: Oxford, 1999; pp 529–598.
27. Blackwell, J.; Vasko, P. D.; Koenig, J. L. *J. Appl. Phys.* **1970**, *41*, 4375–4379.
28. Zerbi, G.; Zoppo, M. D. Vibrational spectra as a probe of structural order/disorder in chain molecules and polymers. In *Modern Polymer Spectroscopy*; Zerbi, G., Ed.; Wiley-VCH: Weinheim, 1999; pp 87–206.
29. Colthup, N. B.; Daly, L. H.; Wiberley, S. E. *Introduction to Infrared and Raman Spectroscopy*, 3rd ed.; Academic: London, 1990.
30. Fengel, D. *Das Papier* **1991**, *45*, 97–102.
31. Michell, A. J. *Carbohydr. Res.* **1993**, *241*, 47–54.
32. Duchesne, I.; Hult, E.-L.; Molin, U.; Daniel, G.; Iversen, T.; Lennholm, H. *Cellulose* **2001**, *8*, 103–111.
33. Fahlén, J.; Salmén, L. *J. Mater. Sci.* **2003**, *38*, 119–126.
34. Hult, E.-L.; Larsson, P. T.; Iversen, T. *Nordic Pulp Pap. Res. J.* **2001**, *16*, 33–39.
35. Åkerholm, M.; Salmén, L. *Polymer* **2001**, *42*, 963–969.
36. Larsson, P. T.; Hult, E.-L.; Wickholm, K.; Pettersson, E.; Iversen, T. *Solid State Nucl. Mag. Reson.* **1999**, *15*, 31–40.
37. Hult, E.-L.; Larsson, P. T.; Iversen, T. *Cellulose* **2000**, *7*, 35–55.
38. Debzi, E. M.; Chanzy, H.; Sugiyama, J.; Tekely, P.; Excoffier, G. *Macromolecules* **1991**, *24*, 6816–6822.